An Advanced Sounder Cloud Contamination Study

WILLIAM L. SMITH AND H. L. HUANG

University of Wisconsin—Madison, Madison, Wisconsin

JOE A. JENNEY

ITT Aerospace/Communications Division, Fort Wayne, Indiana

(Manuscript received 23 June 1995, in final form 12 January 1996)

ABSTRACT

GOES high-resolution visible imagery is used to define the spatial resolution and scan geometry required for an advanced infrared sounder to fly on future polar-orbiting satellites. The definition is based on optimizing the probability of achieving one or more cloud-free infrared sounder fields of view within the footprint of an Advanced Microwave Sounding Unit (AMSU) assumed to have a linear resolution of 64 km. It is found that an instrument with about 8 km linear (10 km circular), or better, resolution that samples nine, or more, spatially independent fields of view within each AMSU footprint is needed to provide a high probability of achieving uncontaminated, by cloud, infrared sounding radiance observations.

1. Introduction

The advanced infrared sounding instruments to be developed for future operational weather and climate satellites will provide the high-spectral-resolution radiance data needed to dramatically improve the vertical resolution and accuracy of space-based temperature and moisture profiles (Smith 1990). However, one limitation of the infrared technique is its inability to sense through dense clouds. Since clouds are generally associated with active weather phenomena, this limitation can be severe, the degree of severity being dependent upon the spatial resolution and scan geometry of the sensor.

Although techniques have been developed to deal with cloud-contaminated fields of view (FOV), these techniques are based on assumptions of cloud optical and geometrical property homogeneity within the FOV of the sensor (Smith 1968; Chahine 1974; Smith and Woolf 1976). Also, both spatial and spectral information must be used to specify the cloud parameters needed to solve the radiative transfer equation for the temperature and moisture profiles. This, in turn, results in an additional degree of nonuniqueness and uncertainty in the solution over that associated with the solution for the clear atmospheric column.

As a consequence of the difficulties in dealing with clouds in the temperature and moisture profile retrieval process, sensor FOV and scan geometry should be designed to achieve as many cloud-free FOVs as practical within the other design constraints of the sensor.

In this study, the trade-off between FOV size and sample density is defined as a function of the probability of achieving cloud-free infrared sounding data on a spatial scale of 64 km. The 64-km spatial scale is the average footprint size of the Advanced Microwave Sounding Unit (AMSU) to fly with the advanced infrared sounder aboard future polar-orbiting satellites. It is also the spatial resolution desired for global numerical weather prediction (NWP) applications of atmospheric soundings from polar-orbiting satellites.

This paper summarizes statistics achieved from several months of midlatitude GOES satellite observations of the Northern Hemisphere winter and spring and the Southern Hemisphere summer and fall seasons. One result reported here is for the entire earth scene within the geostationary satellite's view, which includes the clear and meteorologically benign subtropical high pressure areas. To limit the analysis to the meteorologically significant sounding situations, statistics are also generated only for AMSU size sounding areas that are not totally clear (i.e., partly cloudy and overcast sky conditions). These latter statistics emphasize the sounding conditions in which FOV size and scan geometry are most important. The results of this study strongly support the development of an advanced infrared sounder with an instantaneous area resolution of 70 km^2 (i.e., 8-km square or 10-km-diameter circle), or better, with at least nine spatially independent FOVs per AMSU footprint of about 64 km in linear resolution.

Corresponding author address: Dr. William L. Smith, CIMSS, Space Science and Engineering Center, University of Wisconsin—Madison, 1225 W. Dayton St., Madison, WI 53706.

2. Technique

The data used for this study are from the geostationary satellite imager/sounder, GOES VAS, which has a visible channel with 1-km resolution. The time period of the data is from 29 January–14 March (Northern Hemisphere winter and Southern Hemisphere summer) and 3 April–27 May (Northern Hemisphere spring and Southern Hemisphere fall). The data covers latitudes 45°N–45°S and longitudes 70°–145°W. Only data at satellite subpoint noon (i.e., overhead sun) is used to optimize the use of the high-resolution visible channel for cloud detection.

The clear, partly cloudy, and cloud overcast FOV detection scheme is based on the "spatial coherence method" developed by Coakley and Bretherton (1982). To keep the data processing at a practical level, the 1-km-resolution visible data is spatially averaged over a 4 km × 4 km area and sampled with a spacing of 4 km. Thus, within each 64 km × 64 km sounding area there are a total of 256 resolution elements. In applying the spatial coherence method to these data, the mean radiance and standard deviation about the mean is computed for each 3 × 3 contiguous array of 4-km spaced scan elements. For the visible channel, low reflectance and small standard deviation indicate clear-air FOVs, whereas relatively high reflectance and small standard deviations indicate cloud overcast FOVs. Partly cloudy conditions are associated with intermediate radiance levels and relatively high standard deviations. Figure 1 is an example of the local 3 × 3 mean reflectance and standard deviation for a single 64 km × 64 km area consisting of broken clouds. The clear air reflectances are relatively small over the sea and land, generally less than 6% and 15%, respectively, with local standard deviations less than 3%. Thus, 3 × 3 arrays of clear FOVs are selected on the basis of these criteria. Arrays of cloud overcast FOVs are tagged in a similar manner, but in this case the mean reflectance values are required to be more than 8% greater than the clear-air reflectances with a local standard deviation less than 3%. All FOV arrays not determined to be either cloud-free or cloud overcast are tagged as partly cloudy. As noted by Coakly and Bretherton (1982), this technique will underestimate the number of overcast FOVs because of reflected radiance variability produced by cloud ice/water optical paths in an overcast cloud system. However, this deficiency is not important for this study since the actual cloud amount is determined by a radiation balance condition, rather than by counting cloudy FOVs specified by a threshold condition.

To avoid optically thin "invisible" cirrus cloud, which has relatively small reflectance being classified as clear, an additional check could be performed using infrared "window channel" brightness temperature observations for the same FOV locations of the visible measurements. An infrared test has intentionally not been implemented so that optically thin invisible cirrus cloud is included in the "clear" category. It is desirable to include optically thin cirrus with the clear category, since these types of sounding data are processed in a manner similar to clear-air sounding data. In the optically thin cirrus case, the cirrus cloud optical depth and altitude are computed from the spectral cloud signature information (Smith et al. 1993) and treated as an additional atmospheric absorber in the definition of the profile weighting functions used in the retrieval process (Smith et al. 1990). Since optically thin cirrus is extensive, the inclusion of this type of cloud in the clear category will lead to overestimates of the number of totally clear FOVs, regardless of the sounder FOV size considered. (The reader should keep in mind that "clear" actually denotes clear and optically thin "invisible" cirrus situations whose sounding radiances are treated in the same manner as actual clear radiance data in the profile retrieval process.) The technique used here for distinguishing cloud-free and totally cloud overcast pixels from partly cloudy pixels has been judged to be reasonable through comparisons of the results with the visual inspection of images of the full-resolution (i.e., 1 km) data.

Equivalent cloud-free and cloud overcast reflectance values are obtained for every FOV by bilinear spatial interpolation of the predetermined 3 × 3 arrays of cloud-free and cloud overcast FOV values. Given the observed and interpolated cloud-free and cloud overcast values, the fractional cloud amount A for each 4 km × 4 km visible (V) FOV is defined from the radiation balance expressions

$$A = \frac{V - V_{\text{clr}}}{V_{\text{cld}} - V_{\text{clr}}},$$

where V_{clr} and V_{cld} are the clear and cloud overcast values obtained by the bilinear interpolation of clear and overcast 3 × 3 arrays defined by the process described above. Individual 4-km FOVs are classified as clear if the cloud amount is less than the threshold amount A_T defined as

$$A_T = \frac{3\sigma}{V_{\text{cld}} - V_{\text{clr}}},$$

where σ is the 64-km area mean standard deviation of the clear-sky values as determined by the spatial coherence analysis. If the 64-km linear resolution area mean clear reflectance is an interpolated value (i.e., there were no clear 3 × 3 arrays of 4-km FOVs within the 64-km area), then the 64-km area mean standard deviation σ is assumed to be 1% for the purposes of defining the cloud amount threshold for individual 4-km FOVs.

3. Classification of results

The results of the analysis described above are classified in terms of the following five advanced

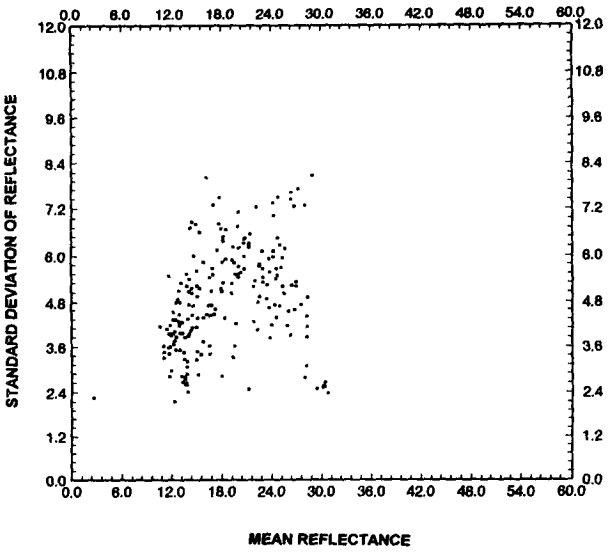

FIG. 1. Spatial coherence diagram computed from a 3 × 3 array of GOES visible reflectance data for a single 64 km × 64 km area consisting of broken clouds.

sounder spatial sampling characteristics within each 64 km × 64 km sounding area:

(a) 3 × 3 array
(b) 2 × 2 array
(c) Nonoverlapping (FOVs contiguous to each other)
(d) 50% gap between FOVs (i.e., undersampled)
(e) Overlapping by 50% (i.e., alias-free sampling)

For each of these spatial sampling conditions the probability of achieving cloud-free conditions is defined in terms of the number of advanced sounder FOVs per sounding area for rectangular FOV sizes of linear dimension: 4, 8, 12, 16, and 32 km.

4. Discussion of results—Clear-air sounding capabilities

Of primary interest here is the probability of achieving cloud-free FOVs within 64 km × 64 km sounding areas as a function of different FOV sizes and scan geometry characteristics. The achievement of one or more cloud-free IR sounding FOVs within an AMSU footprint is required for unambiguous interpretation of the radiance data in terms of atmospheric profiles above the earth's surface independent of any a priori knowledge of the associated cloud conditions.

It was found in this study that the magnitude of the "clear FOV" probabilities depends weakly upon season and latitude zone; that is, the advantages (or disadvantages) of particular FOV characteristics, relative to others, hold true independent of the latitude zone and season considered. Thus, in order to simplify the discussion of the results, the Northern Hemisphere and Southern Hemisphere midlatitude sets for all months have been combined and illustrated in Figs. 2 and 3. Figures 2 and 3 show the results for the probability of achieving totally cloud-free FOVs as a function of the square root of the minimum number of cloud-free FOVs within the sounding area. (The cloud-free signal to noise is proportional to the square root of the number of clear FOVs.) Figure 2 refers to the all-sky condition, whereas Fig. 3 refers to the "nonclear" (i.e., partly cloudy to overcast) AMSU sounding areas, the latter case dramatizing the impact of FOV size and scan geometry on achieving clear-air sounding data in critical meteorological situations. As expected, and as previously suggested by Lee (1993), the scan geometry that yields the highest density of spatially independent samples within a sounding area (i.e., 1/2 FOV overlap) possesses the highest probability of achieving cloud-free measurements. In all cases, the probabilities of sampling cloud-free FOVs decreases rapidly as the size of the FOV increases, particularly for the undersampled scan geometries. Comparing the "alias-free" sampling (i.e., 1/2 FOV overlap) with the contiguous and the 1/2 FOV gap scan geometries, it is seen that there is little significant difference for the achievement of a single clear FOV per AMSU sounding area, particularly for the smaller FOV sizes. However, as the FOV size increases and the desired number of clear FOVs increase, then the probabilities increase significantly with the number density of instantaneous FOVs (i.e., as one approaches alias free sampling). For the practical 3 × 3 or 2 × 2 array scan geometries as proposed for future sounding instruments, the probability of achieving at least one clear FOV per sounding area appears to decrease linearly with linear resolution. It is important to note that in all cases the 8-km resolution 3 × 3 scan geometry is as effective as the 4-km 2 × 2 scan geometry in achieving clear-air sounding data. This result is important in that the 8-km linear resolution would provide significantly higher detector signal to noise than would be achieved with 4-km linear resolution data. It is also noteworthy that in either the 3 × 3 or the 2 × 2 scan geometry considerations, the number of clear FOVs achieved tends to increase linearly with the area resolution (i.e., the square root of the number being proportional to the linear resolution). Since the detector noise is usually proportional to the linear resolution (i.e., square root of the detector area), there is a direct tradeoff between detector noise and cloud noise. Detector noise can be reduced through the averaging of clear FOVs, the loss of sounding radiance signal to noise with increasing spatial resolution is subtle, being proportional to the square root of the linear resolution (i.e., the fourth root of the area), and this loss is compensated by the increasing yield of clear-air soundings. Since cloud noise is much more severe than detector noise, it appears that an optimum design would strive to achieve the highest spatial resolution and sampling density

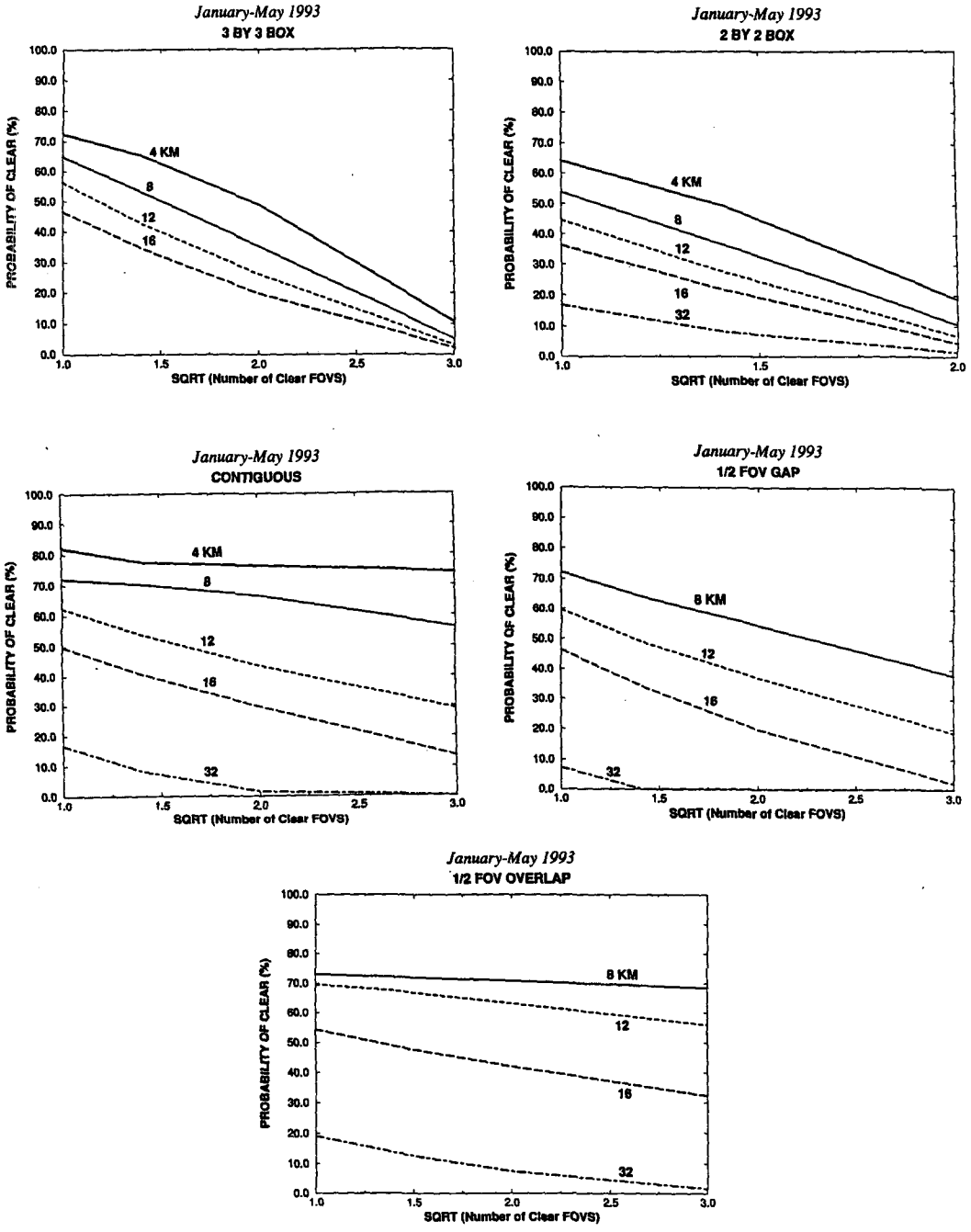

FIG. 2. Probability of finding clear FOVs, having a linear dimension of 4, 8, 12, 16, and 32 km, within a 64 km × 64 km area. The probability is plotted as a function of the square root of the number of clear FOVs, which is proportional to sounding noise. The results are given for five different scan geometries. Results are for January through May 1993. The five scan geometries are (a) 3 × 3 array, (b) 2 × 2 array, (c) contiguous (nonoverlapping), (d) 50% gap between FOVs (undersampled), and (e) overlapping by 50% (alias-free sampling).

(up to the Nyquist limit) as practical, trading off detector noise for clear-air signal. In any case, after considering all significant instrument parameters, it is evident from Figs. 2 and 3 that a reasonable FOV size is about 8 km in linear resolution, implying an instrument with an 8-km rectangular or a 10-km circular FOV design. Significant improvements in clear-air signal to noise can be achieved by increasing the number density of FOVs per sounding area, particularly for the small FOV sizes.

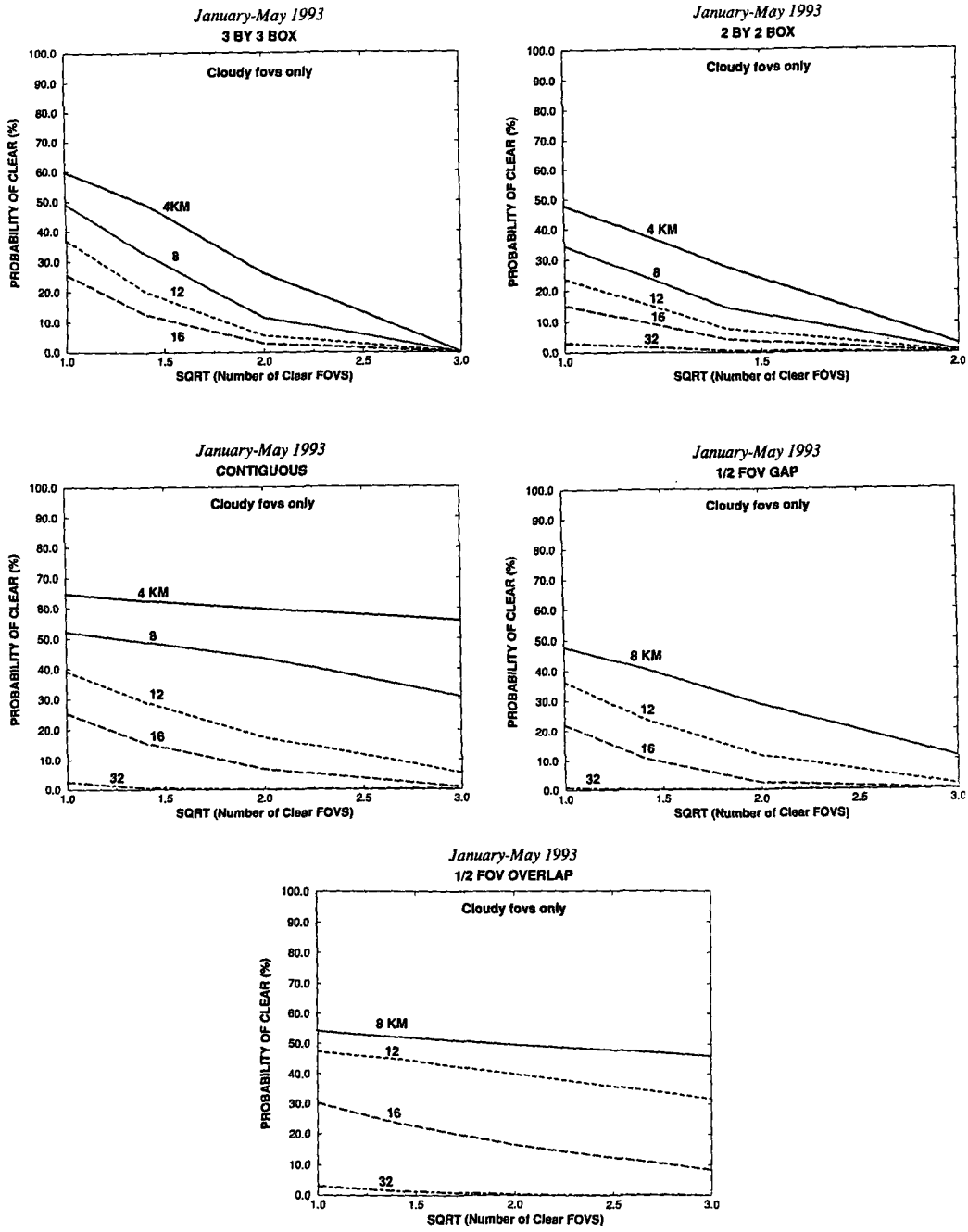

FIG. 3. Same as in Fig. 2 but for cloudy (i.e., partly cloudy to overcast) 64 km × 64 km sounding areas.

One result of studies performed with AVHRR data using multispectral cloud-sensing algorithms (Derrien 1992; Cuomo et al. 1992) is in good agreement with the results obtained here. The AVHRR studies show that reducing the FOV size from 20 to 8 km for a fixed number of FOVs per unit area results in a doubling of the probability to achieve at least one clear FOV within the sampled area. This result is consistent with the results summarized in Figs. 2 and 3.

It is of interest to compare the clear-air sampling capabilities of four advanced sounder FOV sampling designs. The FOV configurations similar to ITS was designed for EUMETSAT as an operational instrument to perform a 3 × 3 sampling within an AMSU footprint with a circular spatial resolution of 10 km. The IASI, under development for the European platform, was originally designed to perform a 2 × 2 array sampling within an AMSU footprint with a circular spatial res-

olution of 18-km diameter, which is equivalent to the 16-km rectangular resolution considered here. (As of December 1995, the IASI FOV has been respecified to be 12 km with a 2 × 2 array sampling within an AMSU footprint.) The AIRS, under development for the EOS PM platform, possesses a 15-km instantaneous FOV, but the continuous, rather than step, scan causes a smearing over a 30-km dimension in the across track (i.e., scan) direction. The AIRS sampling across track is every 15 km such that, for the sake of simplicity, one can assume that the AIRS resolution is equivalent to that of the IASI but with a 3 × 3 measurement density per AMSU sounding area rather than the 2 × 2 measurement density of the IASI. Also included for comparison is a sampling design with 8-km rectangular resolution but with alias-free sampling (i.e., sampling at half the linear resolution of the instrument). An alias-free sampling strategy was first suggested by Lee (1993) as a means to improve the yield of clear-air soundings without increasing spatial resolution and compromising the overall signal to noise of the average cloud-free radiances used to produce the soundings. In the case considered here, the alias-free sampling density of more than 100 FOVs per AMSU footprint could be achieved through the use of a large detector array or by spatial scanning at a relatively high rate. Table 1 below compares the sensing capabilities of these sampling designs for different hemispheres and seasons as based upon the probability analysis described above.

TABLE 1. Probability of achieving clear soundings within a partly cloudy to overcast AMSU footprint for different FOV sampling designs.

Number of clear	3 × 3 (8 km)	2 × 2 (16 km)	3 × 3 (16 km)	Alias-free (8 km)
Northern Hemisphere winter (Jan–Mar)				
>0	29.5	8.9	15.5	34.7
>1	18.7	2.7	7.7	32.7
>3	6.7	0	2.0	30.5
Northern Hemisphere spring (April–May)				
>0	50.2	15.3	26.3	56.7
>1	32.9	4.5	12.7	54.2
>3	11.6	0.1	3.0	51.3
Southern Hemisphere summer (Jan–Mar)				
>0	63.7	22.4	36.1	67.0
>1	44.5	6.5	18.4	65.4
>3	17.0	0.1	4.2	63.5
Southern Hemisphere fall (April–May)				
>0	52.4	14.1	24.0	58.1
>1	32.7	3.5	10.5	55.8
>3	10.3	0	2.1	53.3

The differences in the clear-air sampling capabilities of these four different sampling designs is striking. The 3 × 3 (8 km) sampling design should enable four or more clear FOVs per sounding area with almost the same frequency that the 2 × 2 (16 km) sampling would achieve one or more. This means that in more than 30% of the cases the 3 × 3 (8 km) sampling would tend to have a 2:1 advantage in clear-air signal to noise, all other noise conditions being the same. Most important is the fact that the 3 × 3 (8 km) sampling will provide nearly twice as many clear-air soundings (i.e., able to achieve one or more clear FOVs) than can be achieved by either the 2 × 2 (16 km) or 3 × 3 (16 km) sampling and is nearly equivalent to that achievable with alias-free sampling with the same spatial resolution. On the other hand, it can be seen that alias-free sampling at 8-km resolution might provide even greater clear-air sounding benefits, slightly increasing the total sounding yield at the AMSU resolution and most importantly, enabling a much higher total number of clear FOVs to be achieved within an AMSU footprint.

It is interesting to note that the 8-km resolution alias-free sampling will yield four or more clear-air FOVs with the same frequency that the 3 × 3 (8 km) resolution (i.e., 10 km circular) yields one or more clear-air FOVs. Since the instantaneous noise level of the system is proportional to the square root of the dwell time, the 3 × 3 sampling design could be modified (e.g., by increasing the scan rate) so that there is almost an even trade-off, clear-air signal to noise-wise, between the 3 × 3 sampling design and one in which the scan is almost four times faster to yield alias-free sampling. The very important residual advantage of the alias-free design is that the total yield of clear-air soundings (i.e., one or more clear FOVs) would be increased. However, added complications due to the increased scan speed or the larger detector array size required and the factor-of-4 increase in data rate probably make this an unattractive enhancement of the advanced sounder design.

Finally, it is important to remember that in the absence of completely cloud-free FOVs, the achievement of completely overcast FOVs is important, both for defining the horizontal homogeneity of the cloud within the AMSU footprint and for defining the optical properties of the cloud. In the case of horizontally homogeneous broken cloud, the clear-air radiance can be derived from the spatial variance using the so-called N^* method (Smith 1968). In the case of horizontally homogeneous and optically thick overcast cloud, the sounding above the cloud can be derived with the IR radiances assuming that the height and emissivity of the cloud can be specified. Consequently, all methods for dealing with clouds should benefit from high spatial resolution and high measurement density.

Higher spatial resolution must be traded off against detector signal to noise. However, detector noise is generally much smaller than cloud-induced uncertainties. Moreover, detector noise is usually random so that it can be reduced by spatial averaging. Thus, high spa-

tial resolution and measurement density is important for optimizing the achievement of cloud-free radiances as well as for dealing with the cloud in the retrieval process under heavily clouded atmospheric conditions.

5. Summary and conclusions

This study provides results showing the ability to sense clear-air soundings as a result of instrument resolution and spatial sampling characteristics. The research reported here considered several months of data representing Northern Hemisphere winter and spring and Southern Hemisphere summer and fall conditions. Because of the large geographical area considered and the very large sample of observations used, the results are not expected to change significantly as more seasons are added to the statistics. The dataset and the classification method used are considered to be sufficiently accurate to assess the clear-air (plus invisible cirrus) sounding capabilities of different instrument designs. One result shown here is in excellent agreement with studies performed with AVHRR data using multispectral cloud-sensing algorithms (Derrien 1992; Cuomo et al. 1992), which show that reducing the FOV size from 20 km × 20 km to 8 km × 8 km for a fixed number of FOVs per unit area results in a doubling of the probability to achieve at least one clear FOV within the sampled area. This agreement gives us confidence in the numerous other results provided by this study. One such result is that an alias-free sampling strategy can improve the yield of clear-air soundings without compromising the overall signal to noise of the average cloud-free radiances used to produce the soundings. This is an important consideration to be weighed against the advantages of a higher-spatial-resolution undersampled system and the increased data processing demands of an alias-free system.

The results indicate that an 8-km linear resolution (i.e., 10-km circular resolution) 3 × 3 sampling design would yield almost twice as many clear-air soundings as would be achieved with a 16-km, 2 × 2 sampling. Before any definite conclusion can be drawn regarding the use of the improved alias-free sampling approach, a detailed system tradeoff analysis is required.

Acknowledgments. This study was funded by ITT Aerospace and Communications Division, Fort Wayne, Indiana.

REFERENCES

Chahine, M. T., 1974: Remote sounding of cloudy atmospheres. Part I: The single cloud layer. *J. Atmos. Sci.*, **31,** 233–243.

Coakley, J. A., and F. P. Bretherton, 1982: Cloudcover from high resolution scanner data, detecting and allowing for partially filled fields of view. *J. Geophys. Res.*, **87,** 4917–4932.

Cuomo, V., C. Serio, V. Tramutoli, C. Pietrapertosa, and F. Romano, 1992: Assessing the impact of higher spatial resolution on cloud filtering applied to infrared radiances. Universita della Basilicata Rep., Basilicata, Italy.

Derrien, M., 1992: Influence of the size of field of view on contamination by clouds. Issue 0 contract report to EUMETSAT,

Lee, A. C. L., 1993: IR sounder IFOVs: Small is not necessarily beautiful. Met *O*(RSI) Branch Working Paper No. 46. [Available from Royal Aerospace Establishment, Farnborough, Hants GU14 6TD United Kingdom.]

Smith, W. L., 1968: An improved method for calculating tropospheric temperature and moisture profiles from satellite radiometer measurements. *Mon. Wea. Rev.*, **96,** 387–396.

——, and H. M. Woolf, 1976: The use of eigenvectors of statistical covariance matrices for interpreting satellite sounding radiometer observations. *J. Atmos. Sci.*, **33,** 1127–1140.

——, H. L. Huang, S. A. Ackerman, and H. E. Revercomb, 1990: Sounding through semi-transparent cirrus cloud with high resolution infrared radiance spectra. Preprints, *Fifth Conf. on Satellite Meteorology and Oceanography*, London, England, Amer. Meteor. Soc., 55–59.

——, X. L. Ma, S. A. Ackerman, H. E. Revercomb, and R. O. Knuteson, 1993: Remote sensing cloud properties from high spectral resolution infrared observations. *J. Atmos. Sci.*, **50,** 1708–1720.